$L\beta_{2,15}$ x-ray spectra of elements between $_{41}$Nb and $_{51}$Sb

Pirjo Putila-Mäntylä and Gunnar Graeffe
Department of Physics, Tampere University of Technology, P.O. Box Box 527, SF-33101 Tampere, Finland
(Received 13 July 1988)

The $L\beta_{2,15}$ spectra of elements between $_{41}$Nb and $_{51}$Sb have been measured at high instrumental resolution from solid samples. The satellite structure on the high-energy side of $L\beta_{2,15}$ was resolved and the natural widths of diagram lines were determined. Two different satellite groups due to LM and LN double-hole states were clearly seen. The relative intensity of satellites was examined and it was noticed that the Coster-Kronig channels which create extra holes in the M shell are closed at $_{51}$Sb. A faint structure was observed between the two main groups of satellites after $_{48}$Cd. The L_3O_1 transition falls in this region but it may also be partly the result of triple-hole states.

INTRODUCTION

It has been shown that L_1-L_3M_{45} Coster-Kronig probabilities are very difficult to handle theoretically. Thus experimental information about these transitions is valuable. These transition probabilities can be considered by examining the widths of x-ray diagram lines whose initial state is in L_1 levels.[1-3] The width of an x-ray line of Lorentzian profile is the sum of initial and final state widths. The state width can be calculated from $\Gamma=\hbar(R+C+A)$ where R, C, and A are radiative, Coster-Kronig, and Auger transition probabilities.

Also certain L x-ray-satellite spectra contain information about L_1-L_3M_{45} processes. These satellite structures such as $L\alpha$ satellites are due to LM double-hole states produced by L_1-L_3M_{45} Coster-Kronig (CK) processes or by direct double ionization. The relative intensity and characteristic features of $L\alpha$-satellite spectra between $_{40}$Zr to $_{50}$Sn have been measured already. Also the energies and intensities of $L\alpha$-satellite lines for $_{40}$Zr, $_{45}$Rh, and $_{47}$Ag have been calculated[6] and a good overall agreement was obtained. Besides $L\alpha$, the $L\beta_{2,15}$ high-energy satellite structure is also due to LM (and LN) double-hole states. A few individual spectra of the $L\beta_{2,15}$ line have been published but an overall view in this region has heretofore not been available.

The $L\beta_{2,15}$ (L_3-$N_{4,5}$) x-ray line is interesting in many respects in the elements $_{41}$Nb to $_{51}$Sb. The final state is in the valence band in the elements $_{41}$Nb to $_{45}$Rh and the shape of the $L\beta_{2,15}$ line can be compared to the density of states in the valence band. After $_{46}$Pd the final state is filled and in $_{48}$Cd it is an inner state while O_1 is also filled. Voigt and Lorenzian functions were fitted to the left side and to the peak of the measured $L\beta_{2,15}$ line of elements between Pd and Sb. The precision of our instrument also allows the satellite spectra to be resolved. In previous papers[7,9] the widths of $L\beta_{2,15}$ lines were given, but no details of satellite structures were presented, apart from $_{49}$In.[7] The reported linewidths are thus too wide. In this work the spectral features due to satellites are subtracted and in addition special attention is devoted to the satellite structure on the high-energy side of the diagram line. The relative intensity of the satellite structures is also determined.

EXPERIMENTAL METHOD

The spectra were measured with a high-resolution double-crystal spectrometer. A molybdenum tube was used to excite L emission for all elements other than Pd and Ag; with Pd and Ag a tungsten tube was used. The tube was operated at 40 kV and 40 mA. The spectrometer was equipped with a pair of calcite (211) crystals ($2d=0.606$ nm). The samples of Ru, Rh, Pd, and Sn were 99% pure powder samples. Other samples were spectroscopically pure metal sheets. Their surfaces were cleaned mechanically before introducing them into the vacuum chamber whose pressure was 10^{-1} Pa. The measurements took place at room temperature. The spectrum was recorded stepwise by changing the Bragg angle θ of the second crystal in steps of 17 sec of arc and several successive single spectra were summed up. The experimental arrangement is described in detail in Ref. 4. The rocking curves measured in position $(1,-1)$ have a Lorentzian profile and their full widths at half maximum (FWHM) varied from 0.2 eV (Nb) to 0.4 eV (Sb).

RESULTS

The profile of the lines

The measured spectra of elements $_{41}$Nb to $_{45}$Rh are shown in Fig. 1. In these elements the final state is in the valence band. The shape of the left side of the line should be proportional to the density of the states of d electrons in the valence band. In free atoms the $4d$ shell is filled at $_{46}$Pd. The $L\beta_{2,15}$ spectra from elements $_{46}$Pd to $_{51}$Sb are displayed in Figs. 2–7(a). Theoretical curves were fitted to the measured spectra. For In, Sn, and Sb pure Lorentzian profiles were used, while for Pd, Ag, and Cd the fittings are Voigt functions.

In solids, the $4d$ band for Pd, Ag, and Cd is quite broad and in Pd the calculated Fermi level even falls into the $4d$ band.[10] Therefore the pure Lorentzian profile does not give a good fit for these elements. Nevertheless the fitting for Pd is not very good, which is an indication of the position of the Fermi level.

 ©1989 The American Physical Society

Widths

The measured widths (FWHM) of the elements Nb to Rh and the widths of the fitted curves (Pd to Sb) corrected due to crystal broadening are shown in Table I. The excess width of the $L\beta_{2,15}$ ($L_3N_{4,5}$) line is due to solid-state effects as the final state is the valence band. The narrowing of the line after Rh is a result of filling the bands $4d$ and $5s$. The state width of L_3 ($2p_{3/2}$) is from 2–3 eV in this Z region. Thus we see that the $N_{4,5}$ ($4d$) is very narrow between Cd and Sb. This is due to the fact that $4d$ is a inner state while $4d$ and $5s$ are filled and the Fermi level is far from $4d$ level.

Satellite structure

To resolve the satellite structure the theoretical Voigt and Lorenzian profiles were subtracted from the measured spectra for elements $_{46}$Pd to $_{51}$Sb. The results are shown in Figs. 2–7(b). The effect of resolved satellites seem to be 0.1–0.4 eV in the $L\beta_{2,15}$ linewidths.

Two main groups of satellites are apparent. The first one is located close to the diagram line and the other one 30–50 eV on the high-energy side of the main line. Chen *et al.*[2] have calculated in Ag that an extra vacancy in the M shell shifts the diagram line less than 6 eV. Also in Zr (Ref. 1) the shift should be not more than 6 eV. An extra

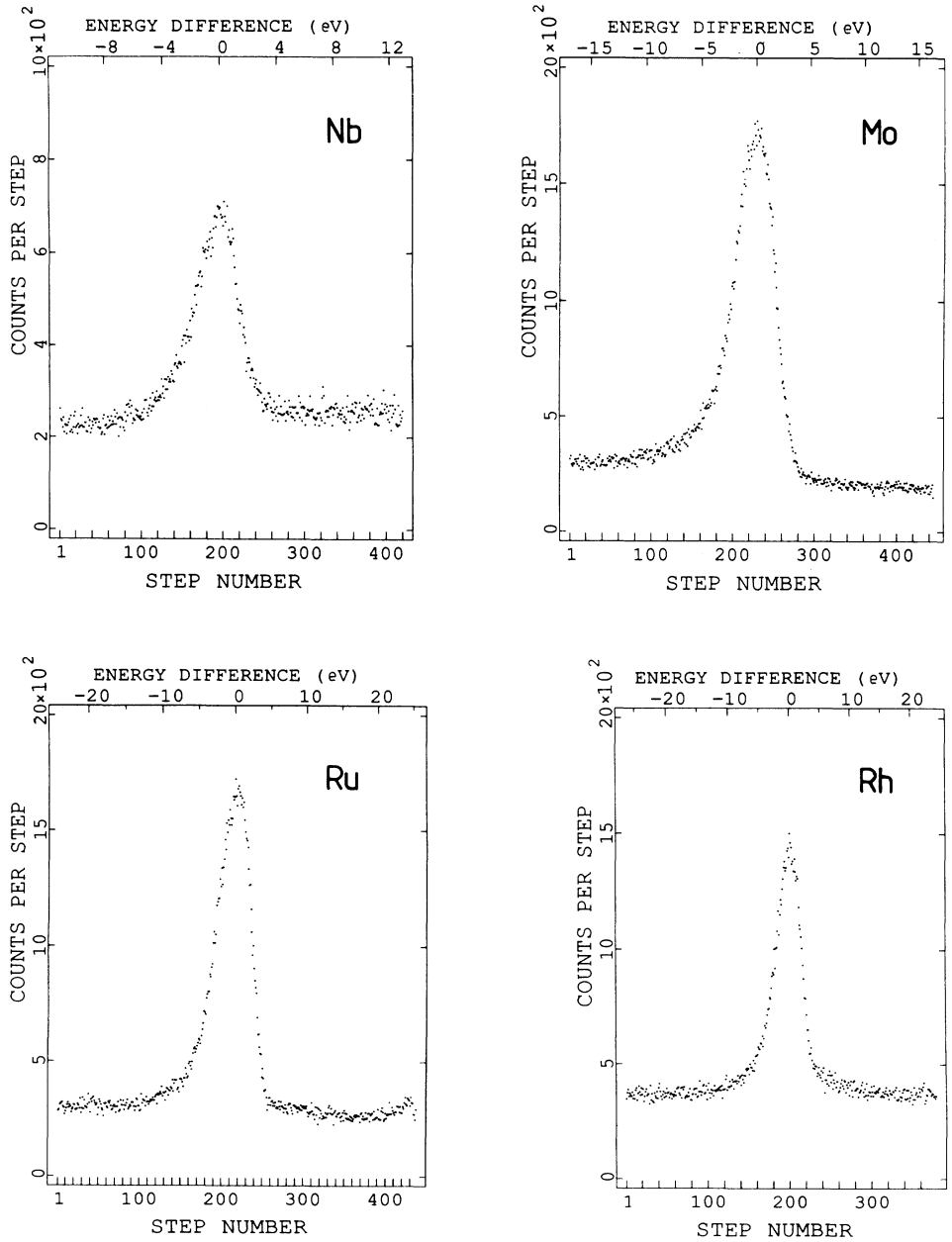

FIG. 1. The $L\beta_{2,15}$ x-ray spectra of elements Nb, Mo, Ru, and Rh. Recording times 900 s/step, 750 s/step, 1050 s/step, and 800/step, respectively. No corrections have been made.

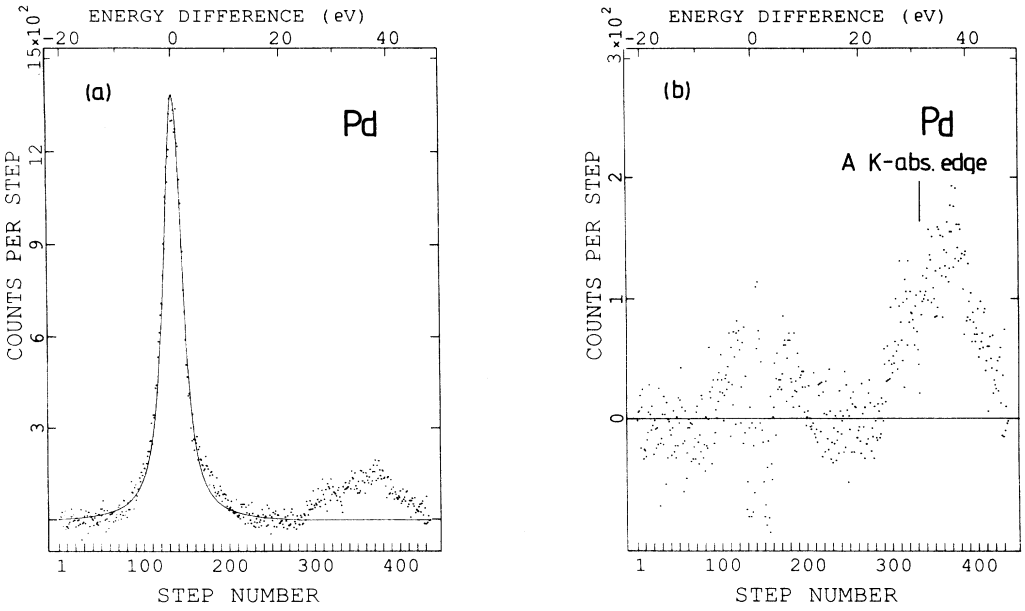

FIG. 2. (a) $L\beta_{2,15}$ x-ray spectrum of Pd recorded at 1000 s/step. Linear background between 480 and 400 counts/step has been subtracted. The total width (Γ) of the fitting is 4.1 eV, the Guassian widths (Γ_G) is 1.8 eV, and the Lorentzian width (Γ_L) is 3.3 eV. (b) Difference spectrum of Pd.

vacancy in the M shell shifts the main line in Ag (Ref. 2) 30–35 eV and in Zr (Ref. 1) 25–30 eV.

Chen *et al.*[2] and Tulkki and Keski-Rahkonen[6] have calculated that there are about 40 possible L_3M_{45}-$M_{45}M_{45}$ satellites in the $L\alpha_{1,2}$ spectra (L_3-$M_{4,5}$) of Ag, Rh, and Zr. As far as we know no theoretical calculations have been carried out for $L\beta_{2,15}$ (L_3-$L_{4,5}$) x-ray spectra. It can be reasonably assumed that the situation is similar there and the structure situated 30–50 eV from the diagram line consists of several tens of satellites arising from LM double-hole states. The interpretation of the structure close to the diagram line is more difficult. There is a strong structure beside the diagram line and this structure has a tail from $_{48}$Cd onwards. The main part of this strong structure is due to LN double-hole states. Also LO double-hole states are possible in this Z

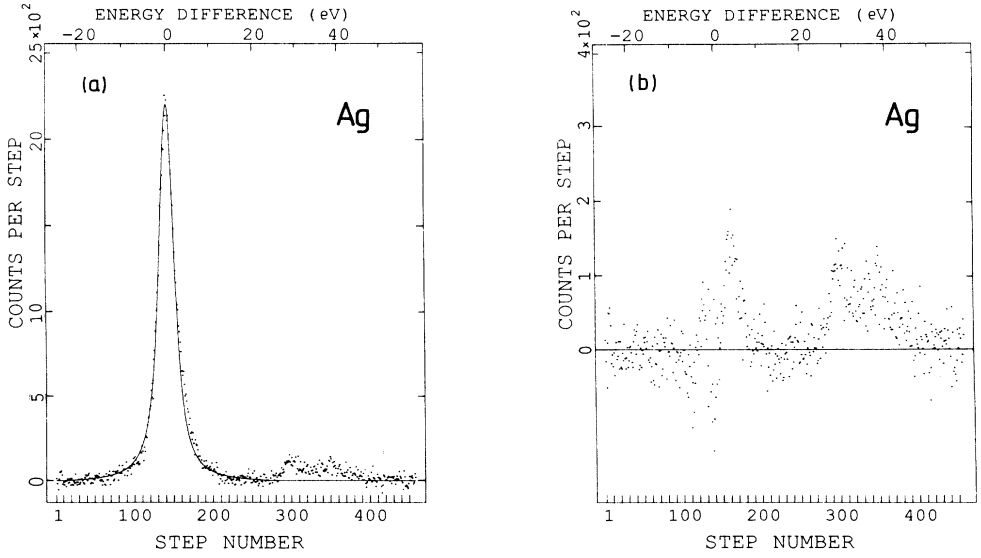

FIG. 3. (a) $L\beta_{2,15}$ spectrum of Ag recorded at 400 s/step. Linear background between 650 and 570 counts/step has been subtracted. $\Gamma = 4.2$ eV, $\Gamma_G = 1.8$ eV, and $\Gamma_L = 3.4$ eV. (b) Difference spectrum of Ag.

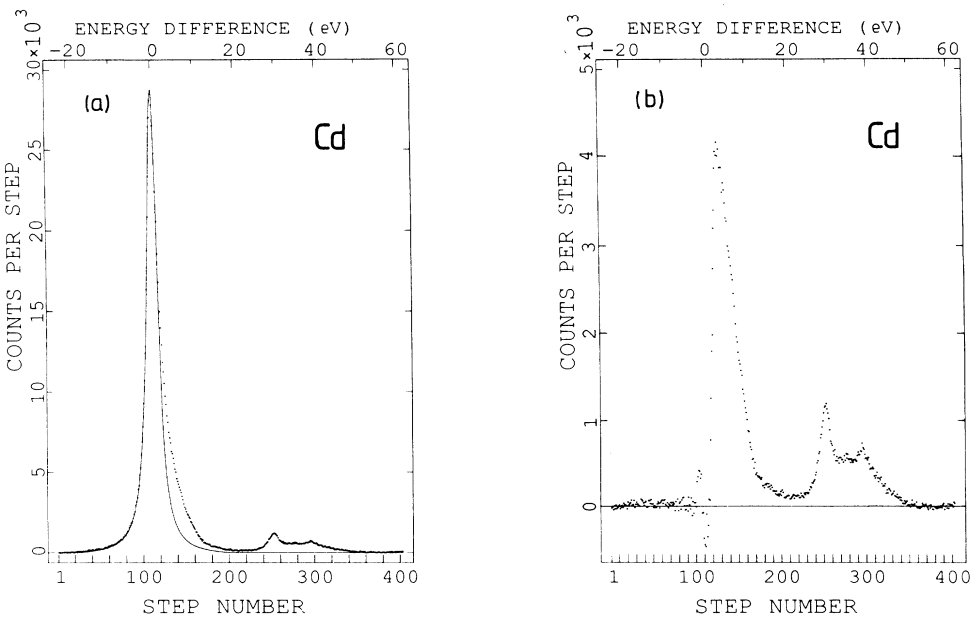

FIG. 4. (a) $L\beta_{2,15}$ spectrum of Cd recorded at 800 s/step. Linear background between 500 and 300 counts/step has been subtracted. $\Gamma = 3.1$ eV, $\Gamma_G = 1.1$ eV, and $\Gamma_L = 2.7$ eV. (b) Difference spectrum of Cd.

region.[11] As mentioned above, an extra hole in the M shell shifts the diagram line ~ 30 eV and in N shell less than 6 eV. The shift due to an extra hole in O shell is even less. Thus we assume that satellites arising from LO and LN double-hole states cannot be totally resolved from the diagram line. According to Ref. 12, $L\beta_7$ (L_3-O_1) transitions fall into the region of the tail mentioned above from $_{49}$In onwards. There are no clear peaks in the spectra but this transition may give some contribution to the tail. Anyway, part of the structure between 11 and 30 eV from the main line might originate from triple-hole states.

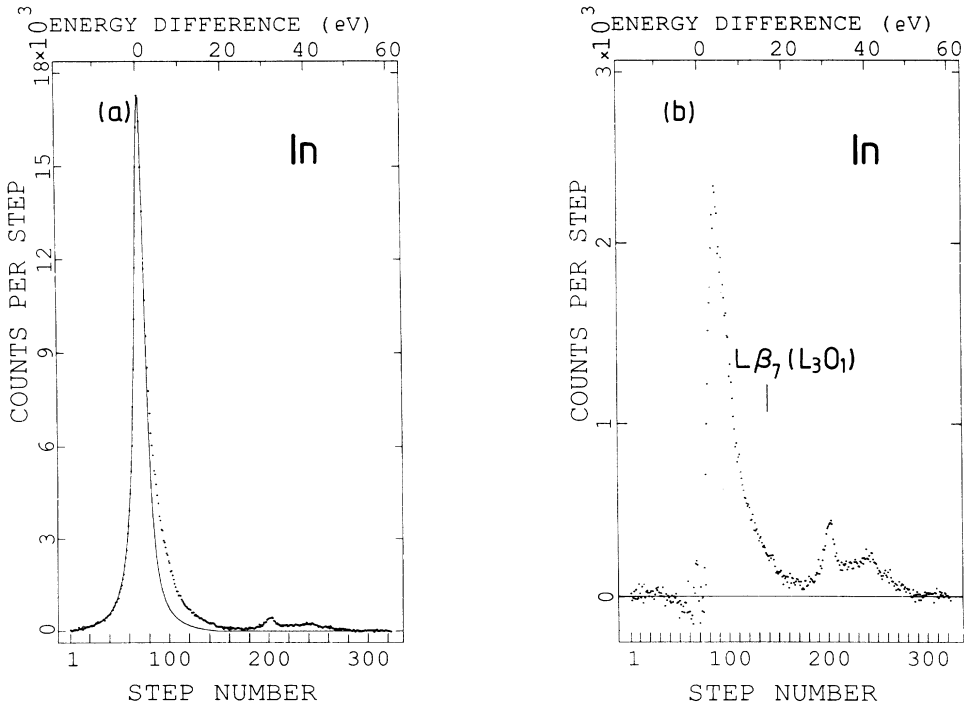

FIG. 5. (a) $L\beta_{2,15}$ spectrum of In recorded at 400 s/step. Linear background between 430 and 300 counts/step has been subtracted. $\Gamma = \Gamma_L = 3.0$ eV. (b) Difference spectrum of In.

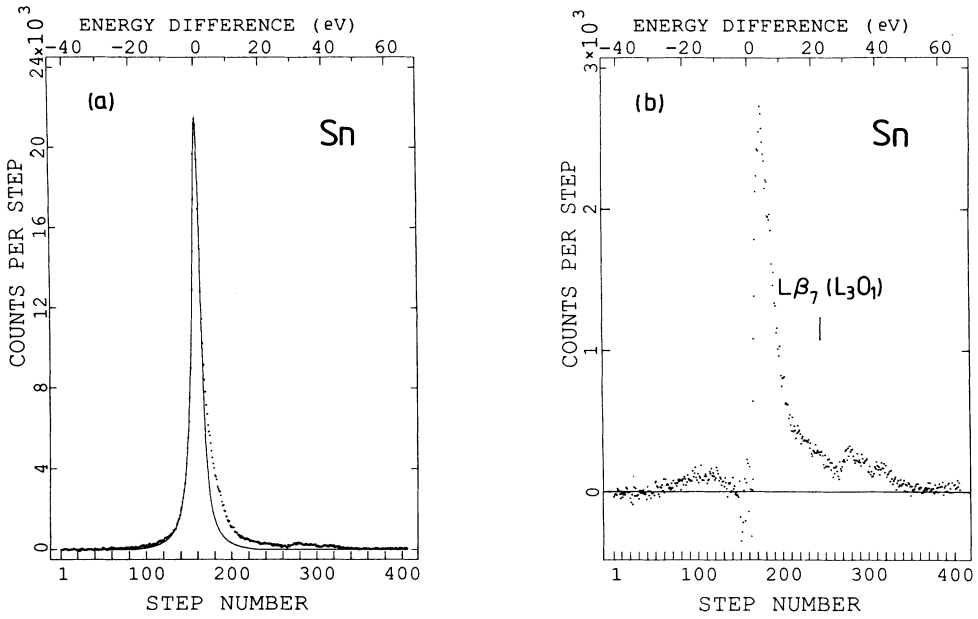

FIG. 6. (a) $L\beta_{2,15}$ spectrum of Sn recorded at 800 s/step. Linear background between 990 to 740 counts/step has been subtracted. $\Gamma = \Gamma_L = 3.2$ eV. (b) Difference spectrum of Sn.

Satellite intensities

The relative intensity of different satellite groups was determined. The difficulty in choosing the background is the great uncertainty in the intensity measurement, especially in those spectra whose statistics are not very good. For example, in our measurement for elements Ru to Ag, the uncertainty of intensities is mainly due to different choices of the satellite backgrounds. In Ru and Rh the intensity was determined from a single measurement (200 s/step). The relative intensities of the satellites due to *LM* double-hole states are displayed in Fig. 8. The relative intensity of the Pd satellite structure have to be corrected for the argon *K* absorption edge which falls in the middle of the satellite structure (an argon-methane gas mixture was used in the detector).

After Rh the relative intensity of $L\beta_{2,15}$ high-energy satellites diminishes and in Sb the structure has vanished, only a weak intensity (1%) is left. This satellite structure is a result of *LM* double-hole states. These states are

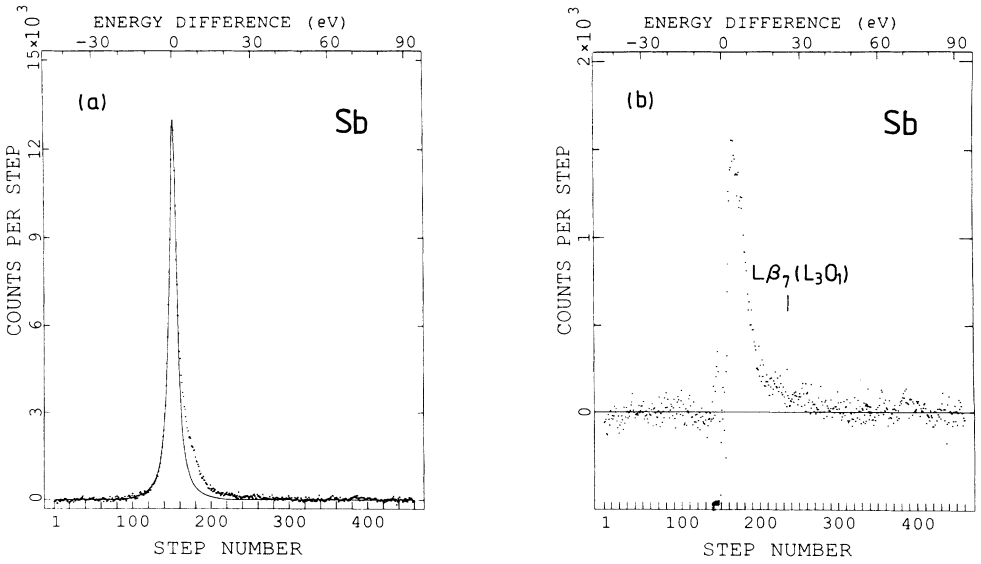

FIG. 7. (a) $L\beta_{2,15}$ spectrum of Sb recorded 600 s/step. Linear background between 2100 to 2000 counts/step has been subtracted. $\Gamma = \Gamma_L = 3.4$ eV. (b) Difference spectrum of Sb.

TABLE I. Natural linewidths of the measured $L\beta_{2,15}$ lines (in eV) and the electronic configurations of corresponding atoms.

Element	FWHM of $L\beta_{2,15}$[a]	Configuration
$_{41}$Nb	3.4	$4d^4 5s$
$_{42}$Mo	4.1	$4d^5 5s$
$_{44}$Ru	5.3	$4d^7 5s$
$_{45}$Rh	4.5	$4d^8 5s$
$_{46}$Pd	3.8	$4d^{10}$
$_{47}$Ag	3.8 (3.72[b])	$4d^{10}5s$
$_{48}$Cd	2.7	$4d^{10}5s^2$
$_{49}$In	2.6	$4d^{10}5s^2 5p$
$_{50}$Sn	2.8	$4d^{10}5s^2 5p^2$
$_{51}$Sb	3.0	$4d^{10}5s^2 5p^3$

[a]Instrumental error is less than 0.2 eV.
[b]Reference 2.

created by Coster-Kronig processes and by direct double ionization. For photon impact,[6] the ratio of the double- to single-ionization cross section decreases roughly as Z^2. Thus for successive elements, such as Sn and Sb, this ratio changes only slightly. Hence the weak intensity over background in Sb is probably due to LM double-hole states produced by direct double ionization. We conclude therefore that $L_1L_3M_{45}$ Coster-Kronig processes become forbidden at $_{51}$Sb in the solid state.

It has been calculated[11] that in free atoms the L_1-L_3M_{45} CK transitions are no longer possible at $_{50}$Sn. In Sn and Sb the final state of the $L\beta_{2,15}$ transition is very narrow. The atom-solid shift is 8–9 eV in these elements.[13] While the binding energy in solids is lower, the $L_1L_3M_{45}$ Coster-Kronig energy is higher in solids and these transitions probably become forbidden later in solids than in atoms. The total relative intensity of all satellites between 1 and 30 eV is displayed in Table II, column I. It does not change much. This total structure has been divided into two components. The first component (column II) is the satellites due to an extra N shell vacancy. It is difficult to say up to how far this first component should extend since no exact calculations have been made. The tail was resolved from the main structure and its intensity is presented in column III. The main contribution in this tail is probably the $L\beta_7$ (L_3O_1) line and the possibility of triple-hole states should be discussed. The intensity of this "tail" situated between about 11 and 30 eV from the $L\beta_{2,15}$ diagram line seems to grow as a function of Z.

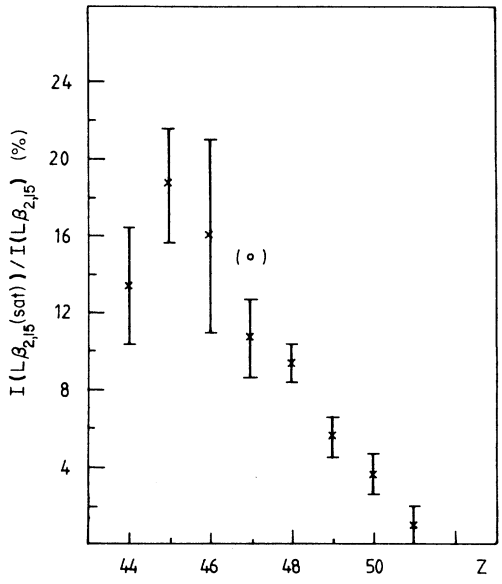

FIG. 8. Relative intensity of $L\beta_{2,15}$ satellite structure arising from LM double-hole states. For $Z=46$ corrected for argon K absorption edge. The value from Ref. 2 is also shown (○).

CONCLUSIONS

The widths of $L\beta_{2,15}$ (L_3N_{45}) x-ray lines for elements $Z=41$ to 51 are reported. The filling of valence and conduction bands is seen in the linewidth (narrowing with increasing element number). The satellite structure due to an extra hole in the M shell decreases after $_{45}$Rh and has essentially vanished at $_{51}$Sb. This indicates that in solids L_1-$L_3M_{4,5}$ the Coster-Kronig channel is closed at Sb. The intensity of satellites due to an extra N-shell vacancy does not seem to change much.

TABLE II. The relative intensity of $L\beta_{2,15}$ satellite structures: (1) the structure between 1 to about 30 eV from the diagram line, (2) satellites close to $L\beta_{2,15}$ (due to LN double holes), (3) structure between ~11 to 30 eV from the diagram line, and (4) satellites between ~30 to 50 eV from the main line (due to LM double holes).

Element	a	b	c	d
$_{44}$Ru				13±3
$_{45}$Rh				19±3
$_{46}$Pd				16±5[a]
$_{47}$Ag				11±2
$_{48}$Cd	22	20±1	2.1±1	9.4±1
$_{49}$In	22	19±1	3.0±1	5.6±1
$_{50}$Sn	23	19±1	3.6±1	3.6±1
$_{51}$Sb	22	18±1	4.0±1	1.0±1

[a]Corrected due to K absorbtion edge of argon.

[1]M. O. Krause, F. W. Wuilleumier, and C. W. Nestor, Phys. Rev. A **6**, 871 (1972).
[2]M. H. Chen, B. Crasemann, M. Aoyagi, and H. Mark, Phys. Rev. A **15**, 2312 (1977).
[3]P. Putila-Mäntylä, M. Ohno, and G. Graeffe, J. Phys. B **17**, 1735 (1984).
[4]H. Juslen, M. Pessa, and G. Graeffe, Phys. Rev. A **19**, 196 (1979).
[5]P. Putila, H. Juslen, M. Pessa, and G. Graeffe, Phys. Scr. **20**, 41 (1979).
[6]J. Tulkki and O. Keski-Rahkonen, Phys. Rev. A **24**, 849 (1981).
[7]P. Putila-Mäntylä and G. Graeffe, Phys. Rev. A **35**, 673 (1987).
[8]L. G. Parratt, Phys. Rev. **54**, 99 (1938).
[9]M. Ohno, P. Putila-Mäntylä, and G. Graeffe, J. Phys. B **17**, 1747 (1984).
[10]V. L. Moruzzi, J. F. Janak, and A. R. Williams, *Calculated Electronic Properties of Metals* (Pergamon, New York, 1978), pp. 144–155.
[11]M. H. Chen, B. Crasemann, and H. Mark, At. Data Nucl. Data Tables **24**, 13 (1978).
[12]J. A. Bearden, Rev. Mod. Phys. **39**, 78 (1967).
[13]P. Putila-Mäntylä, M. Ohno, and G. Graeffe, J. Phys. B **16**, 3503 (1983).